Available online at www.sciencedirect.com

ScienceDirect

Procedia Technology 17 (2014) 343 – 350

Procedia Technology

Conference on Electronics, Telecommunications and Computers – CETC 2013

On the Feasibility of Indoor Light Energy Harvesting for Wireless Sensor Networks

Carlos Carvalho[a,b,*], Nuno Paulino[b,c]

[a] *Instituto Politécnico de Lisboa (IPL), Instituto Superior de Engenharia de Lisboa (ISEL), Área Departamental de Engenharia de Electrónica e Telecomunicações e de Computadores (ADEETC), Rua Conselheiro Emídio Navarro, nº1, 1959-007 Lisboa, Portugal*

[b] *UNINOVA/CTS, Campus FCT/UNL, 2829-516 Caparica, Portugal*

[c] *Universidade Nova de Lisboa (UNL), Faculdade de Ciências e Tecnologia (FCT), Departamento de Engenharia Electrotécnica (DEE), Campus FCT/UNL, 2829-516 Caparica, Portugal*

Abstract

This paper presents the important issues about the design of a low cost, micro power, indoor light energy harvesting system to supply a node of a wireless sensor network (WSN). Possible technology options, available for the photovoltaic (PV) cells, are discussed. Light power and irradiance measurements, in a real indoor environment, are performed and results are presented. From these results, a possible solution for cell sizing is described.

Peer-review under responsibility of ISEL – Instituto Superior de Engenharia de Lisboa, Lisbon, PORTUGAL.

Keywords: Energy harvesting; Irradiance measurements; Light energy; Light power measurements; PV cells; Wireless sensor networks.

1. Introduction

The ability of electronic circuits to obtain their source of power from the surrounding environment is a feature that has gained increased attention [1], either for sensor networks [2], or embedded systems [3]. Sensor networks that only rely on power grid connections are limited to a relatively small range of applications, as network nodes can never be too far from a power outlet. For pervasive operation, relying on the grid is a limiting factor. The use of batteries allows for freedom about sensor distribution, but as their stored charge gets depleted, they need to be

* Corresponding author. Tel.: +351-21-8317239; fax: +351-21-8317236.
E-mail address: cfc@cedet.isel.ipl.pt

Peer-review under responsibility of ISEL – Instituto Superior de Engenharia de Lisboa, Lisbon, PORTUGAL.
doi:10.1016/j.protcy.2014.10.206

replaced. This can be a problem if a large number of sensors are deployed, especially in places that are difficult to reach. Thus, the simple operation of battery replacement can become expensive and burdensome.

To tackle these limitations and achieve indefinite operation, electronic devices must obtain their energy directly from the surrounding environment. This kind of procedure is commonly known as energy harvesting. Besides its pervasive character, energy harvesting is both ecological and thrifty, because sensor systems do not need batteries to power the circuits, and will not contribute to environmental pollution caused by disposing of the depleted batteries, or even their manufacturing, in the first place. In economical terms, this represents cost reduction both in devices and maintenance procedures.

Although there are different possible energy sources that can be harvested to power electronic applications, the context described in this paper uses light energy because, comparing all sources, this is the one that shows the highest energy density by volume unit, for low-power systems [4].

Using indoor light to power an electronic application is an increased challenge, because the levels of available light energy inside buildings are much lower than those that can be obtained outside.

2. Light energy

Light is an electromagnetic wave, comprising an interval of frequencies in which it is visible. In the lower end of this interval, light tends to be red. As the frequency increases, light goes through the known colors, and in the upper end, it gets violet. Thus, light is bounded by infrared and ultraviolet.

The light spectrum outside the atmosphere, also known as the 5800 K blackbody, has the designation of AM0 (Air Mass 0), meaning “zero atmospheres”. This is the standard used to characterize PV cells that are used in space, to power satellites.

The sunlight, after penetrating the atmosphere, at sea level, perpendicularly to the surface of the Earth, has a spectrum which is referred to as AM1 (one atmosphere). AM1 is useful for estimating the performance of solar cells in equatorial and tropical regions. The index “1” is related to the angle of solar incidence, which is minimal in this situation.

In most places, the incidence of the Sun has a different angle than in the Equator, and sunlight must cross a greater amount of atmosphere. As such, this spectrum is referred to as AM1.5 (one and a half atmospheres), on a clear day. This value is the standard test condition (STC) for terrestrial PV panels. For higher latitudes, there are more Air Mass indexes, used for higher incidence angles, above 60º. These indexes can go up to AM38 in the polar zones, where the incident angle is close to 90º. In any of these cases, atmospheric pollution has influence over the irradiated energy, limiting the amount reaching the surface of the Earth.

The light energy is different according to each wavelength. The spectral power density of the solar radiation is shown in Fig. 1, where the top curve is the solar spectrum just outside the atmosphere.

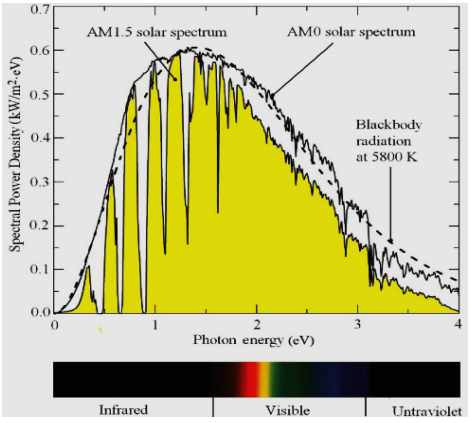

Fig. 1. Spectral power density of solar radiation [5].

The total power density in this zone is 1.366 kW/m^2, which is known as the solar constant. The curve filled with yellow is the standardized solar spectrum on the surface of Earth, for performance evaluation of PV cells (AM1.5). The standard power density in these conditions is about 1 kW/m^2, across the whole wavelength spectrum.

The dashed curve is the solar radiation spectrum at the position of the Earth by modeling the Sun as a blackbody radiator at 5800 K. As shown, the solar spectrum just outside the atmosphere, the AM0 spectrum, matches well with the blackbody radiation spectrum at 5800 K, diluted by the distance from the Sun to the Earth. The relation with human vision of color spectrum is shown in the bar beneath the spectrum. As shown in Fig. 1, only about one half of the solar radiation power is visible [5].

2.1. Indoor light energy harvesting

In indoor light energy harvesting applications, the amount of available light energy is small, it can vary significantly and it has a different nature than in outdoors, because natural light is attenuated and can be mixed with artificial light. The literature reports available indoor irradiances ranging from one tenth of the maximum Sun intensity [6] to about 0.833 W/m^2 (100 lux converted to W/m^2 using [7]) in a lightly dimmed room [8], or 10 W/m^2, when the PV cells are placed very close to lamps [9].

The conversion principle indicated in [7], considers the nature of the light spectrum in indoor environments, where there is a predominance of artificial light, provided by light bulbs or light tubes. The latter have such a spectrum, which leads to the application of the conversion from lux to W/m^2 to be given by

$$E_{rad}(\mathrm{W/m^2}) = \frac{E_{rad}(\mathrm{lux})}{120}. \tag{1}$$

Given the unit of light intensity, the lux (lx), according to some authors, there is another correspondence between the amount of power by unit of area and the amount of incident light, and it is defined under the relation that 1 kW/m^2 = 683 klx, i.e. 1 lx = 1/683 W/m^2. This conversion is used, for example, in [10], and unlike (1), it does not take into account the fact that the light has an indoors spectral pattern. According to [10], the level of indoor lighting is still enough to power electronic applications, namely from overhead fluorescent lights, with 34 W of power.

3. Photovoltaic (PV) cells

The key element for light energy harvesting is the PV cell, which is basically a photodiode. This solid state device converts light energy directly to electrical energy without the use of any moving parts.

When the PV cell is illuminated, its output behaves like a current source with a voltage limiter. PV cells are characterized by three main parameters: the maximum power point (MPP), the open circuit voltage (V_{OC}) and the short circuit current (I_{SC}). The PV cell can be modelled by an equivalent electrical circuit, which is shown in Fig. 2, with the parameters of the equivalent circuit (I_1, R_P and R_S) characterizing it. The parameters of the diode (D) also play an important role according to the amount of light illuminating the PV cell.

In Fig. 3, it is shown a typical plot of the power and the output current (i_{out}) generated by a PV cell (the same as the one used in [11]), letting know how these functions look like, *versus* the output voltage of the PV cell, v_{out}.

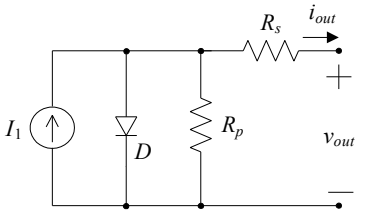

Fig. 2. Equivalent electrical circuit of a PV cell.

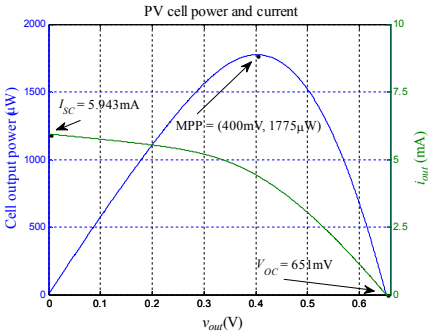

Fig. 3. Example of typical current and power curves, as a function of the output voltage, for maximum illumination.

The cell power function is obtained by multiplying the output voltage, v_{out}, by the output current, i_{out}. The maximum power point (MPP) is achieved with an output voltage greater than half of the open circuit voltage, unlike in common voltage sources, according to their Thévenin equivalent. The percentage of the V_{OC} that corresponds to the MPP is about 71% to 78% [12], being this value dependent on light and temperature. As it can be seen from this survey reference [12], the maximum power point tracking (MPPT) issue is an active area of research.

The output current of the PV cell (i_{out}) is related to the remaining elements of the model, according to

$$i_{out} = I_1 - I_S\left(e^{q\frac{v_{out}+R_s i_{out}}{nkT}} - 1\right) - \frac{v_{out}+R_s i_{out}}{R_p}. \quad (2)$$

In this equation, I_S is the limit of the current in the diode under high reverse bias, known as "dark saturation current", i.e. the diode leakage current density in the absence of light. Also, q is the electron elementary charge ($1.60217657 \times 10^{-19}$ C) and k is the Boltzmann constant ($1.380648813 \times 10^{-23}$ J/K). T is the ambient temperature, expressed in K. The factor n is the emission (or ideality) coefficient, which equals 1 for an ideal diode.

The efficiency of the most common PV cells is still relatively low, at about 20% [13]. Under indoor environments, amorphous silicon (a-Si) PV cells can have efficiencies up to about 7% [10].

In order to try to reduce the production costs, it is possible to use PV cell technologies with lower efficiencies, but that also have lower manufacturing costs, resulting however in a larger area for the PV cell, for the same output power level. Using amorphous silicon PV cells is an example of such a trade-off, in which costs are lower, but at the expense of a larger area to obtain the same level of output power. Next, in Fig. 4, it is illustrated the differences of the power densities measured on crystalline silicon (SOLEMS 09/030/012) and amorphous silicon (Schott ASI2Oi05/055) PV panels, when different light sources are used to generate the same illumination level [14].

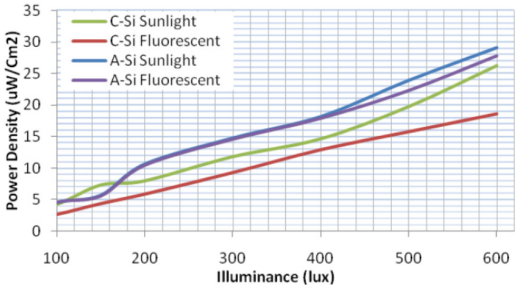

Fig. 4. Power densities of light sources at various illumination levels [14].

In indoor environments, as opposed to crystalline silicon (c-Si) PV cells, amorphous silicon PV cells do not suffer a strong reduction in their power density, when the source of light changes from sunlight to fluorescent lights. Thus, this evidence is indicating that the amorphous silicon-based cells are more suited for indoor applications.

Moreover, if the overall cost is one of the most meaningful factors, this option will have to be seriously taken into account to preserve commercial competitiveness, because a-Si cells are less expensive.

4. Indoor light energy availability study and results

Before starting the design of an indoor environment energy harvesting system, it is necessary to have a real understanding of the available light power in such an environment. In order to assess the amount of available light in an indoor environment, a set of measurements was performed.

There are some literature references, some of which have been indicated in this text, in which light measurements were also performed. Examples of such, are in [8], [10], or [14]. However, in order to have a true perspective of the light availability in indoor environments that can be found in typical *campus* facilities, at the geographical location where this work was developed, it was decided to perform these measurements. This study can, eventually, be extrapolated to similar indoor situations. A S120B silicon light sensor [15] was used, connected to a measuring device, the Thorlabs PM100 Digital Power Meter Console [16]. This device allows for separate light power readouts over a set of wavelength widths. The available wavelengths for the present case were centered at 450 nm, 500 nm, 550 nm, 600 nm and 650 nm. Optical band-pass filters with 40 nm of width were used to perform these partial measurements [17]. Afterwards, these partials were combined into a single light irradiance value, which is a lower bound approximation, given the small gaps that are not covered, between the bands of the band-pass filters.

The measurements were performed in four locations inside an office room, as the one sketched in Fig. 5. These locations cover most of the cases that a light energy harvester would find in an indoor environment. These four locations correspond to L_1 and L_2, and in each, at two different distances (h) from the ceiling lamps.

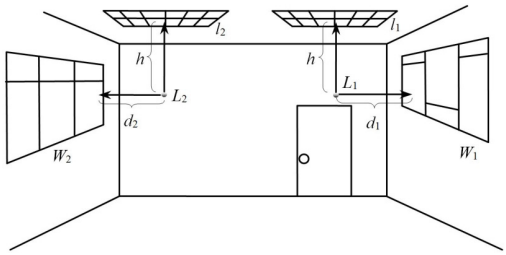

Fig. 5. Schematic picture of the room where the indoor measurements took place.

In Fig. 5, l_1 and l_2 are the lamps on the ceiling; h is the distance between those lamps and the sensor [located either at L_1 (under l_1), or L_2 (under l_2)]; W_1 and W_2 are the windows of the office room; d_1 and d_2 are the horizontal distances between each of the windows and the sensor (located at L_1 or L_2, respectively). The values of the previous dimensions are $d_1 = 2.3$ m; $d_2 = 2.4$ m; $h = 1$ m or 2 m; area of $W_1 = 1 \times 2 = 2$ m^2; area of $W_2 = 1.25 \times 2.6 = 3.25$ m^2.

The room is located at latitude 38º45'25''N and longitude 9º7'2''W. Window W_1 is orientated to East and the light entering from it is not as bright as the one that enters through W_2 (orientated to West), because the latter is directly at the façade of the building, while the former is not. Each of the lamps l_1 and l_2 is composed by two fluorescent light tubes, with a power of 36 W each. Other type of lamps can lead to different measurement results.

The light sensor can be oriented upwards to l_1 or l_2 (↑), to W_1 (→) or to W_2 (←). To each position is assigned an index, to help to identify it. A measurement taken outdoors is identified with index 0. The complete set of positions is listed next, in Table 1. In each measurement, the light sensor orientation was slightly adjusted in order to maximize the received light power, as it would occur in a real energy harvesting situation. The measurements were performed during two days (January, the 30th of 2012 and February, the 23rd of 2012), at different times of the day, having sunny weather outside. Since in wintertime, outdoor (natural) light is weaker than in the rest of the year, these measurements can be considered as worst cases.

Table 1. Positions where the measurements took place, referring to Fig. 5.

Position	h	Location	Orientation
0	O U T D O O R		
1	1 m	L_1	↑
2			→ W_1
3			W_2←
4		L_2	↑
5			→ W_1
6			W_2←
7	2 m	L_1	↑
8			→ W_1
9			W_2←
10		L_2	↑
11			→ W_1
12			W_2←

Outdoor measurements were also performed, in order to have a reference value, which can be compared to the values measured indoor. The indoor measurements, depending on the time of the day, comprehended natural light, natural and artificial light, or only artificial light.

The whole set of measured values is listed in Table 2. This table presents the total power value measured by the light sensor and the corresponding calculated irradiance. At 19h00m, it was already dark outside, so naturally, the measurements only account for the artificial light inside the room.

Table 2. List of measured values, having sunny weather outside (except at 19h00m).

Position Index	Jan, 30th 2012 10h30m		Jan, 30th 2012 12h30m		Feb, 23rd 2012 16h30m		Feb, 23rd 2012 19h00m	
	P_{total} (μW)	Irradiance (W/m^2)	P_{total} (μW)	Irradiance (W/m^2)	P_{total} (μW)	Irradiance (W/m^2)	P_{total} (μW)	Irradiance (W/m^2)
0	20840	294	24080	340	16640	235	-	-
1	179.86	2.54	172.54	2.43	157.35	2.22	152.37	2.15
2	129.31	1.82	85.28	1.20	75.59	1.07	-	-
3	50.34	0.71	35.10	0.50	17.24	0.24	-	-
4	168.82	2.38	163.88	2.31	159.73	2.25	158.82	2.24
5	20.36	0.29	15.94	0.22	14.23	0.20	-	-
6	162.26	2.29	81.92	1.16	17.20	0.24	-	-
7	72.41	1.02	63.04	0.89	55.31	0.78	54.25	0.77
8	65.31	0.92	18.78	0.26	9.99	0.14	-	-
9	44.00	0.62	23.62	0.33	9.14	0.13	-	-
10	64.31	0.91	56.90	0.80	51.37	0.72	51.60	0.73
11	35.73	0.50	19.50	0.28	12.51	0.18	-	-
12	187.23	2.64	61.31	0.86	18.80	0.27	-	-

4.1. Discussion

These measurements help to get an *in loco* realistic idea about the amount of light energy that can be found in a typical *campus* office environment. The measurements were performed at different times of the day, considered different types of light (representing the conditions of that place) and are generic (not committed to any type of cell).

According to the summarized data in Table 2, the value of 0.13 W/m^2 is the worst case and corresponds to the lowest irradiance value found in this indoor environment. According to (1), this irradiance is 15.6 lux. Using only artificial light, the typical irradiance value was about 0.7 W/m^2, which is 84 lux. Normally, in datasheets of commercially available PV cells, the lowest irradiance, about which there is information, is 100 lux or 200 lux.

4.2. Solution approach

The silicon PV cells presented in Section 3, according to [14], are only two in a universe of types and manufacturers. However, these serve to have an idea about the difference in area, when using the c-Si or a-Si

technology. Instead of the SOLEMS 09/030/012, the data about a similar cell, the SOLEMS 09/055/020 (c-Si), is used. The other cell used in this comparison is the Schott ASI2Oi05/055 (a-Si), as in Section 3. Due to the available datasheet information, let us assume that both PV cells are irradiated with 200 lux, according to (1), 1.67 W/m^2. This is the lowest irradiance value, about which there is datasheet information, in order to establish a direct comparison of performance between these two PV cells. The area of the c-Si cell is 5.5 cm × 2.0 cm = 11 cm^2, while for the a-Si this is 5.5 cm × 1.35 cm = 7.425 cm^2. At the MPP, the first cell can provide 32.4 μW and the second 31 μW. These values are very similar, but the a-Si cell needs a smaller area, given the irradiance serving as a reference for both.

This comparison serves to confirm that at indoor light levels, and given the specific light spectrum, the a-Si PV cell is the one that should be preferred. If an indoor light energy harvesting system is to power a WSN node, one common management technique, is duty-cycling: the node will sleep for most of the time, only waking up for a short period, in order to transmit some bytes of information regarding the data acquired by the sensor. The working regime can be described according to the following equation:

$$P_{average} = P_{working}(\delta) + P_{sleeping}(1-\delta), \tag{3}$$

in which, δ is the duty-cycle, $P_{average}$ is the average power consumed during a whole cycle, $P_{working}$ is the power that the node consumes while in operation and $P_{sleeping}$ is the power that the node consumes when in the idle state.

Let us consider an energy harvesting system of the same kind as the one in [11]. Its management circuit, using MPPT consumes, on average, 10 μW working the whole time to harvest energy. Let us also consider the use of a transmitter circuit like the one used in [18], needing 448 μs to transmit 14 bytes of data, encompassing protocol and payload information, at a rate of 250 kbit/s. When idle, this transmitter consumes 1.5 μW and when transmitting, it consumes 63 mW. If this system is to make one transmission every hour, its duty-cycle is

$$\delta = \frac{448\,\mu\text{s}}{1\,\text{hour}} = \frac{448\,\mu\text{s}}{3600\,\text{s}} \cong 1.24\times10^{-7}. \tag{4}$$

The average power needed to operate for the period of one hour is

$$P_{average} = (63\times10^{-3} + 10\times10^{-6})(1.24\times10^{-7}) + (1.5\times10^{-6} + 10\times10^{-6})(1-1.24\times10^{-7}) \cong 11.51\,\mu\text{W}, \tag{5}$$

and the energy required is

$$E = P_{average}\times\Delta t \cong 11.51\,\mu\text{W}\times3600\,\text{s} = 41.43\,\text{mJ}. \tag{6}$$

This energy must be stored in a supercapacitor to be provided when needed, according to the relation

$$E = 1/2\times C\times\Delta V_C^2 = 41.43\,\text{mJ}, \tag{7}$$

where C is the capacitance value and V_C is the supercapacitor voltage. The capacitance of such devices can reach values as high as 3000 F [19], but for this application, a lower value should be selected due to body size restrictions.

As an estimation given the available data, and considering that, for the selected PV cell, the available power scales approximately linearly with irradiance, for the worst case, at the MPP, the minimum required area would be

$$A = 7.425\,\text{cm}^2\left[\frac{11.51\,\mu\text{W}}{\frac{31\,\mu\text{W}}{\left(200\,\text{lux}\,/\,15.6\,\text{lux}\right)}}\right] \cong 35.3\,\text{cm}^2. \tag{8}$$

5. Conclusions

This paper discussed the issues about indoor light energy harvesting. Light energy was characterized, as well as the electrical model for PV cells. From different technologies, amorphous silicon showed to have a better vocation to harvest indoor light energy. Light power and irradiance measurements were performed in order to check about the real energy availability in an indoor scenario. A commercial PV cell, selected from literature, was used as example. Based on its datasheet features, its sizing was established to meet the requirements of a WSN node, demanding an average power level of 11.51 μW, considering the worst case reported by the indoor measurements.

Acknowledgements

The authors wish to thank to Dr[a]. Paula Louro and Dr. Miguel Fernandes, from ISEL-ADEETC, for lending the measurement equipment and its accessories.

This work was supported by grant SFRH/PROTEC/67683/2010, financially supported by the IPL – Instituto Politécnico de Lisboa.

References

[1] Paradiso, J. A., Starner, T. (2005). Energy scavenging for mobile and wireless electronics, *IEEE Pervasive Computing*, Vol. 4, No. 1, January-March 2005, pp. 18-27.

[2] Chou, P. H., Park, C. (2005). Energy-efficient platform designs for real-world wireless sensing applications, *in Proceedings of the ICCAD 2005 - IEEE/ACM International Conference on Computer Aided Design*, 6-10 November 2005, pp. 913-920.

[3] Raghunathan, V., Chou, P. H. (2006). Design and Power Management of Energy Harvesting Embedded Systems, *in Proceedings of the ISLPED 2006 - International Symposium on Low Power Electronics and Design*, 4-6 October 2006, pp. 369-374.

[4] Chalasani, S., Conrad, J. M. (2008). A survey of energy harvesting sources for embedded systems, *in Proceedings of the IEEE Southeastcon 2008*, 3-6 April 2008, pp. 442-447.

[5] Chen, C. J. (2011). *Physics of Solar Energy*. John Wiley & Sons, Inc., Hoboken, New Jersey.

[6] Rabaey, J., Burghardt, F., Steingart, D., Seeman, M., Wright, P. (2007). Energy Harvesting - A Systems Perspective, *in Proceedings of the IEDM 2007 - IEEE International Electron Devices Meeting*, 10-12 December 2007, pp. 363-366.

[7] Randall, J. F., Jacot, J. (2003). Is AM1.5 applicable in practice? Modelling eight photovoltaic materials with respect to light intensity and two spectra. *Renewable Energy*, Vol. 28, No. 12, October 2003, pp. 1851-1864.

[8] Weddel, A. S., Merret, G. V., Al-Hashimi, B. M. (2012). Photovoltaic sample-and-hold circuit enabling MPPT indoors for low-power systems. *IEEE Transactions on Circuits and Systems I: Regular papers*, Vol. 59, No. 6, June 2012, pp. 1196-1204.

[9] Hande, A., Polk, T., Walker, W., Bhatia, D. (2007). Indoor solar energy harvesting for sensor network router nodes. *Microprocessors and Microsystems*, Vol. 31, No. 6, September 2007, pp. 420-432.

[10] Nasiri, A., Zabalawi, S. A., Mandic, G. (2009). Indoor Power Harvesting Using Photovoltaic Cells for Low-Power Applications. *IEEE Transactions on Industrial Electronics*, Vol. 56, No. 11, November 2009, pp. 4502-4509.

[11] Carvalho, C., Lavareda, G., Lameiro, J., Paulino, N. (2011). A step-up μ-power converter for solar energy harvesting applications, using Hill Climbing maximum power point tracking, *in Proceedings of the IEEE International Symposium on Circuits and Systems (ISCAS 2011)*, 15-18 May 2011, pp. 1924-1927.

[12] Esram, T., Chapman, P. L. (2007). Comparison of Photovoltaic Array Maximum Power Point Tracking Techniques. *IEEE Transactions on Energy Conversion*, Vol. 22, No. 2, June 2007, pp. 439-449.

[13] Rabaey, J., Burghardt, F., Steingart, D., Seeman, M., Wright, P. (2007). Energy Harvesting - A Systems Perspective, *in Proceedings of the IEEE International Electron Devices Meeting (IEDM 2007)*, 10-12 December 2007, pp. 363-366.

[14] Wang, W. S., O'Donnell, T., Wang, N., Hayes, M., O'Flynn, B., O'Mathuna, C. (2010). Design considerations of sub-mW indoor light energy harvesting for wireless sensor systems. *ACM Journal on Emerging Technologies in Computing Systems (JETC)*, Vol. 6, No. 2, June 2010, article 6.

[15] ThorLabs Instrumentation. S120B - Standard Power Sensor, Si, 400 - 1100 nm, 50 mW [Online]. Available: http://www.thorlabs.com/thorproduct.cfm?partnumber=S120B.

[16] ThorLabs Instrumentation. PM 100 Operating manual [Online]. Available: http://www.thorlabs.com/Thorcat/12200/12271-D02.pdf.

[17] ThorLabs Instrumentation. FB450-40 - Ø1 Bandpass Filter, CWL = 450 ± 8 nm, FWHM = 40 ± 8 nm [Online]. Available: http://www.thorlabs.com/thorproduct.cfm?partnumber=FB450-40.

[18] Thewes, M., Scholl, G., Li, X. (2012). Wireless energy autonomous sensor networks for automobile safety systems, *in Proceedings of the 9th International Multi-Conference on Systems, Signals and Devices (SSD 2012)*, 20-23 March 2012, pp. 1-5.

[19] Maxwell Technologies. Datasheet K2 series ultracapacitors [Online]. Available: http://www.maxwell.com/products/ultracapacitors/docs/datasheet_k2_series_1015370.pdf.